



ELSEVIER

Contents lists available at ScienceDirect

Journal of Magnetism and Magnetic Materials

journal homepage: www.elsevier.com/locate/jmmm

Low temperature combustion synthesis and magnetostructural properties of Co–Mn nanoferrites

A.B. Salunkhe^{a,*}, V.M. Khot^a, M.R. Phadatare^a, N.D. Thorat^a, R.S. Joshi^b, H.M. Yadav^a, S.H. Pawar^a^a Centre for Interdisciplinary Research, D. Y. Patil University, Kolhapur 416006, Maharashtra, India^b The Magnetism Group, Department of Physics, Indian Institute of Science, Bangalore 560012, India

ARTICLE INFO

Article history:

Received 16 March 2013

Received in revised form

16 July 2013

Available online 11 October 2013

Keywords:

Combustion synthesis

Co–Mn ferrite nanoparticle

Structural and magnetic property

ABSTRACT

In the present work, $\text{Co}_{1-x}\text{Mn}_x\text{Fe}_2\text{O}_4$ nanoparticles were synthesized by the low-temperature auto-combustion method. The thermal decomposition process was investigated by means of differential and thermal gravimetric analysis (TG-DTA) that showed the precursor yield the final product above 450 °C. The phase purity and crystal lattice symmetry were estimated from X-ray diffraction (XRD). Micro-structural features observed by scanning electron microscopy (SEM) demonstrates that the fine clustered particles were formed with an increase in average grain size with Mn^{2+} content. Fourier transform infrared spectroscopy (FTIR) study confirms the formation of spinel ferrite. Room temperature magnetization measurements showed that the magnetization M_s increases from 29 to 60 emu/g and H_c increases from 13 to 28 Oe with increase in Mn^{2+} content, which implies that these materials may be applicable for magnetic data storage and recording media.

© 2013 Elsevier B.V. All rights reserved.

1. Introduction

Magnetic nanoparticles have become more and more important in a variety of electronic, magnetic, and catalytic applications, because of their interesting soft magnetic properties, high frequency application and easy preparation method [1,2]. Ferrites are well-known magnetic nanomaterials intensively studied as a recording media due to their superior physical properties. Magnetic properties of ferrites can be changed by substituting various kinds of M^{2+} (Zn^{2+} , Mg^{2+} , Mn^{2+} , Ni^{2+} , Co^{2+} , Fe^{2+} , etc.) among divalent cations by introducing a relatively small amount of transition metal ions. Among the various ferrite magnetic nanoparticles; Cobalt ferrite is one of the ferrimagnetic oxide with spinel structure, which has many unique properties, such as high coercivity (H_c), high Curie temperature (~ 520 °C), temperature specific saturation magnetization (M_s), chemical stability, and mechanical hardness, and large magnetocrystalline anisotropy. Additionally, this material exhibits a significant higher magnetostriction than metallic Fe or Ni. [3,4] Furthermore due to high magnetomechanical coupling, high sensitivity to stress and magnetostriction properties, cobalt substituted spinel ferrites has received more attention for magnetomechanical stress and torque

sensors and actuator applications [5]. The substitution of metal ions like Mn^{2+} into the cobalt ferrite has been proposed by many researchers to modify the magnetic and magneto mechanical properties. In particular, extensive studies of Mn-doped CoFe_2O_4 have been conducted, which showed that the substitution of Mn for Fe decreases the Curie temperature, magnetic anisotropy, and magnetostriction coefficient [6–11].

Conventionally, Mn doped cobalt ferrites are synthesized by the various methods like sol-gel [12], the powder ceramic technique [13], solid state reaction [14,15], combustion [16], co-precipitation [17] etc. Bham and Joy et al. have reported that $\text{Co}_{1-x}\text{Mn}_x\text{Fe}_2\text{O}_4$ ($0 \leq x \leq 0.4$) nanoparticles prepared by solid state reaction exhibit higher magnetostriction at relatively lower magnetic fields at optimum Mn content $x=0.3$ [14,15]. A model in which the Mn^{3+} ions enter into the O_h sites and some of the Co^{2+} ions occupy the T_d sites, has been used to explain these results, but further clarification is still needed [7,18]. However, Co–Mn ferrite single phase can only be formed after being calcinated at high temperature with these methods. Furthermore, as an annealing process at a temperature higher than 600 °C is always necessary for all wet-chemical synthesis methods, the negative effect on reducing the media noise, which is brought by the accompanied particle growth, aggregation and coarseness of Co–Mn nanoferrites, seems to be unavoidable. In order to overcome the shortcoming of these methods, the low-temperature auto-combustion process is employed. Besides, compared with wet-chemical methods, simple process, inexpensive cost, short reaction time and energy consuming

* Corresponding author. Tel.: +91 231 2601202, 2601235; fax: +91 231 2601595.

E-mail addresses: salunkhe_ab@rediffmail.com (A.B. Salunkhe), pawar_s_h@yahoo.com (S.H. Pawar).

are all the advantages of this method. Some other advantages of combustion synthesis are (1) use of relatively simple equipment, (2) formation of high-purity products, (3) stabilization of metastable phases, and (4) formation of virtually any size and shape products, and (5) powders prepared by low-temperature auto-combustion method have good sinterability with a homogeneous composition.

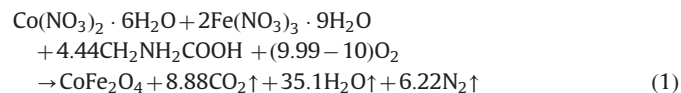
In the present investigation, an attempt has been made to synthesis Co–Mn ferrite nanocrystalline powder by the low-temperature auto-combustion method.

The TG-DT analysis, FTIR, XRD, SEM, EDAX, TEM and VSM techniques were used to study thermal evolution of the precursor, as well as the microstructure, morphology and magnetic properties of as-synthesized Co–Mn ferrite nanopowder respectively.

2. Experimental

2.1. Synthesis

Cobalt manganese ferrite ($\text{Co}_{1-x}\text{Mn}_x\text{Fe}_2\text{O}_4$ ($0 \leq x \leq 0.4$)) nanoparticles with different Mn^{2+} contents x were prepared by the combustion method. Analytical grade cobalt nitrate ($\text{Co}(\text{NO}_3)_2 \cdot 6\text{H}_2\text{O}$), manganese nitrate ($\text{Mn}(\text{NO}_3)_2 \cdot 6\text{H}_2\text{O}$), ferric nitrate ($\text{Fe}(\text{NO}_3)_3 \cdot 9\text{H}_2\text{O}$) and glycine ($\text{CH}_2\text{NH}_2\text{COOH}$) have been used as source for the preparation of $\text{Co}_{1-x}\text{Mn}_x\text{Fe}_2\text{O}_4$ nanoparticles. The reactions procedure was carried out in air atmosphere without protection of nitrogen or inert gas. The detailed synthesis procedure is discussed elsewhere [19,20]. As burnt powder was used for further characterizations. The possible chemical reaction for $\text{Co}_{1-x}\text{Mn}_x\text{Fe}_2\text{O}_4$ at $x=0$ is given in equation



2.2. Characterization

The precursor gel was characterized for TGA by means of SDT 2960 simultaneous DSC-TG-DTA instruments U.S.A. at the heating rate of $10^\circ\text{C}/\text{min}$ in an air stream. Phase of as prepared samples was confirmed by X-ray diffraction pattern. XRD patterns recorded on Philips PW-3710 automated XRD equipped with a crystal monochromatic employing $\text{Cr-K}\alpha$ radiation of wavelength 2.28970 \AA . Fourier transform infrared spectra (FTIR) were recorded in the wavenumber of $300\text{--}800 \text{ cm}^{-1}$ on a Perkin-Elmer apparatus (model V755). Morphological analysis was carried out using SEM (JEOL JSM 6360 with EDAX). EDAX was used for compositional analysis of the samples. The magnetic characterizations were carried out by VSM (Lake Shore 7307 model) under the applied field of $\pm 9000 \text{ Oe}$ at room temperature. TEM images were recorded on a Philips apparatus (model CM 200).

3. Results and discussion

3.1. TG-DT analysis on the combustion process

The autocatalytic nature of the combustion process in which the nitrate ions act as an oxidizer while the glycine plays the role of a reducer was investigated by TG-DTA measurements and the results are presented in Fig. 1. The experimental DTA curve shows an endothermic peak appears at $\sim 137.4^\circ\text{C}$ and two exothermic peaks at ~ 171.3 and $\sim 440.6^\circ\text{C}$, respectively. Obviously, the endothermic peak locating at 137.4°C originates from the vaporization process of the inner water contained in precursor gel. The TG curve shows three weight loss processes at temperatures

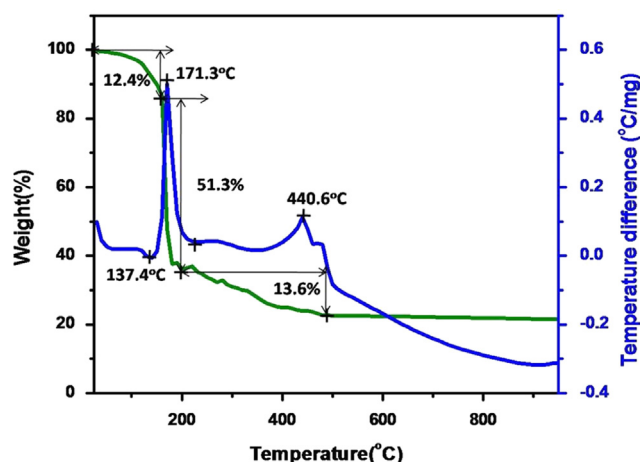


Fig. 1. TG-DT curve of precursors gel.

27–160 $^\circ\text{C}$ (12.4%), 160–200 $^\circ\text{C}$ (51.3%) and 200–500 $^\circ\text{C}$ (13.6%) with a total weight loss of 77.3%. Around the first exothermic peak, 171.3°C , the corresponding TG curve demonstrates a drastic weight loss. The combinational results indicate the occurrence of an auto-combustion process during the oxidative decomposition of the precursor gel. As for the broad exothermic band scaling from ~ 430 to $\sim 500^\circ\text{C}$ and peaking at 440.6°C , which is accompanied with a weight loss of $\sim 4\%$, should come from the burning of the residual organic components. The overall weight loss in the two exothermic reaction processes is $\sim 77.3\%$ of the precursor gel, which is in good agreement with theoretical weight loss calculated from Eq. 1.

3.2. Structure and phase analysis

The crystallinity and structure of the as prepared particles were confirmed by XRD patterns. XRD patterns of all samples prepared by a combustion method are shown in Fig. 2. The samples show all the characteristic reflections of ferrite material with most intense (3 1 1) reflection which confirms the formation of cubic spinel structure (Fig. 2).

All XRD patterns were well indexed using the JCPDS card No. 22-1086 [21] and 74-2403 [22]. The diffractogram exhibits sharp lines, which indicates that the sample has high crystallinity. From the XRD data, the crystallite size (D_c) of as prepared $\text{Co}_{1-x}\text{Mn}_x\text{Fe}_2\text{O}_4$ nanoparticles was calculated using Scherrer Equation [22]

$$D_c = \frac{K\lambda}{\beta \cos \theta} \quad (2)$$

where, β is breadth of the observed diffraction line at its half intensity maximum, K is the so-called shape factor, which usually takes a value of about 0.9 and λ is the wavelength of the X-ray source used in XRD. From Fig. 2 it is observed that as a content of Mn^{2+} increases the lattice constant steadily increases from 8.37 \AA to 8.41 \AA thereby obeying Vegard's law [15]. This linear increase in lattice constant (a) with Mn^{2+} content ' x ' can be explained on the basis of a difference in ionic radii of Co^{2+} , Fe^{3+} , and Mn^{2+} . The smaller ionic radius of Co^{2+} (0.78 \AA) and Fe^{3+} (0.64 \AA) ions are replaced by larger Mn^{2+} (0.83 \AA) ions; consequently the lattice parameter increases because of expansion of unit cell dimension. When small sized Co^{2+} ions substituted with large sized Mn^{2+} ions, the spinel cobalt ferrite will eventually expand. Doping of Mn^{2+} ions in spinel type structure will induce uniform strain in the lattice as the material is elastically deformed. This effect causes the lattice plane spacing to change and the diffraction peaks shifts to lower 2θ positions (Fig. 2b).

Download English Version:

<https://daneshyari.com/en/article/8157510>

Download Persian Version:

<https://daneshyari.com/article/8157510>

[Daneshyari.com](https://daneshyari.com)